AIAA JOURNAL
Vol. 36, No. 2, February 1998

Updated Lagrangian Formulation of a Flat Triangular Element for Thin Laminated Shells

P. Mohan* and Rakesh K. Kapania†
Virginia Polytechnic Institute and State University, Blacksburg, Virginia 24061-0203

An updated Lagrangian formulation of a three-node flat triangular shell element is presented for geometrically nonlinear analysis of laminated plates and shells. The flat shell element is obtained by combining the discrete Kirchhoff theory plate bending element and a membrane element that is similar to the Allman element but a derivative of the linear strain triangular element. Results are presented for large-rotation static response analysis of a cantilever beam under end moment, cylindrical shell under pinching and stretching loads, a hemispherical shell under pinching and stretching loads, and a ring plate under a line load; for dynamic response analysis of a cylindrical panel; and for thermal postbuckling analysis of an imperfect square plate and a cylindrical panel. To estimate the accuracy of the present formulation in predicting the nonlinear response of large flexible structures, static analysis of an apex-loaded circular arch is performed. The arch is a building block of a large inflatable structure. The results are in good agreement with those available in the existing literature and those obtained using the commercial finite element software ABAQUS, demonstrating the accuracy of the present formulation.

I. Introduction

THE two most widely adopted approaches in the finite element analysis of shells are use of curved shell elements based on a suitable shell theory and approximation of the curved structure by an assemblage of flat shell elements in which the membrane-bending coupling is brought about as a result of material anisotropy and transformation of the element stiffness matrices computed in a local coordinate system to the global coordinate system prior to assembly. The curved shell elements can be computationally very expensive, especially in the case of nonlinear analysis, because of the complexity of the formulation and the need to compute the curvature information. Flat shell elements are more attractive because of their simplicity and the ease with which they can be built from already-existing familiar membrane and plate bending elements. Though a large number of elements are required to accurately model curved structures, the analysis is computationally less expensive because of extremely simple formulation.

Updated Lagrangian formulations have been predominantly used in the flat shell formulations available in the existing literature. In an updated Lagrangian formulation, all of the variables are referred to a known configuration, the reference configuration, which is updated continuously during the deformation process. If the rigid-body modes are removed from the total or incremental displacements, the resulting deformational translations and rotations are very small and hence a linearized incremental formulation[1] can be used. In a linearized incremental formulation, the stresses are computed using linear strain-displacement relations. The tangent stiffness matrix contains only the linear stiffness matrix and the initial stress matrix. The stiffness matrices resulting from the nonlinear terms in the strain-displacement relations are neglected, resulting in very economical analysis. If the rigid-body modes are not removed, all nonlinear terms in the strain-displacement relations will have to be considered for computing the stresses and the tangent stiffness matrix.

A three-node flat triangular shell element was introduced by Argyris et al.[2] for nonlinear elastic stability problems. This formulation, denoted as the natural mode technique, is based on decomposing the displacements into rigid-body and straining modes, which are exhibited naturally by any structure undergoing deformation.

Horrigmoe and Bergan[3] presented flat triangular and quadrilateral shell elements based on a hybrid stress model for static analysis of isotropic plates and shells. They employed a linearized updated Lagrangian formulation in which the rigid-body modes are removed from the total displacements. The initial stress matrix was obtained using a lower-order interpolation than that used for the linear stiffness matrix.

Bathe and Ho[4] presented a three-node flat triangular shell element for static analysis of isotropic plates and shells. This element was obtained by combining the discrete Kirchhoff theory (DKT) plate bending element of Batoz et al.[5] and the well-known constant strain triangular (CST) plane stress element. Bathe and Ho[4] used a linearized updated Lagrangian formulation in which the undeformed coordinates are used to obtain the strain-displacement matrices for all times. The membrane stresses and internal forces are computed from total displacements as was done by Horrigmoe and Bergen[3] whereas the curvatures and the bending moments are computed from incremental displacements and updated at the end of each increment. Bathe and Ho[4] also used a lower-order interpolation to compute the initial stress matrix. Because they used a linearized incremental formulation without removing the rigid-body rotations from the total or incremental displacements, their formulation is restricted to moderate incremental rotations.

The restriction in the formulation of Bathe and Ho[4] was overcome by Hsiao[6] by removing the rigid-body modes from the total displacements. Both the membrane and the bending internal force vectors are obtained from the total deformational translations and rotations in the updated Lagrangian formulation used by Hsiao.[6]

Fafard et al.[7] presented a six-node flat triangular shell element called DLTP for static analysis of isotropic plates and shells. Their flat shell element is obtained by combining the six-node DKT plate bending element (DKTP) of Dhatt et al.[8] and the well-known linear strain triangular (LST) plane stress element. Though the interpolations used for the transverse displacement and the normal rotations in the DKTP element are one order higher than those used in the DKT element, the accuracy of the DKTP element was found to be of the same order as that of the DKT element.[8] This is because in both formulations the rotation of the normal to the undeformed mid-surface of the element about the element edges is assumed to vary linearly along the edges.

Fafard et al.[7] presented two updated Lagrangian formulations. The first, termed ULF1, is a total Lagrangian formulation within

Received March 4, 1997; presented as Paper 97-1233 at the AIAA/ASME/ASCE/AHS/ASC 38th Structures, Structural Dynamics, and Materials Conference and Exhibit, Kissimmee, FL, April 7–10, 1997; revision received Aug. 15, 1997; accepted for publication Sept. 24, 1997.

*Graduate Research Assistant, Department of Aerospace and Ocean Engineering.

†Professor, Department of Aerospace and Ocean Engineering. Associate Fellow AIAA.

each step, with the configuration at the beginning of the step taken as the reference configuration for the next step. The second, termed ULF2, is a fully updated Lagrangian formulation with the estimated configuration at the end of each iteration taken as the reference configuration for the next iteration. In ULF1, all nonlinearities are considered in the computation of stresses and the tangent stiffness matrix. In ULF2, a linearized incremental formulation is used but the stresses are computed using nonlinear strain-displacement relations as in ULF1. Fafard et al.[7] studied the importance of using lower-order interpolations for the transverse displacement (w) to compute the nonlinear terms in the Green–Lagrange strains and the initial stress matrix. They found that a linear interpolation for w is preferable with DLTP and that the DCT element (combination of the DKT and CST elements), which suffers from severe locking when a cubic interpolation is used for w, could be made softer by using a linear interpolation for w. Fafard et al.[7] also found that, in the case of ULF2, the solution failed to converge when very large initial increments were used.

Chen[9] presented a three-node flat triangular shell element obtained by combining the CST element and the plate bending element of Morley[10] for large displacement elastoplastic analysis of isotropic plates and shells. Chen used the von Kármán theory of large deflection and adopted the Lagrangian description to describe the deformation of the element. Chen presented numerical examples that involved only small rotations. Peric and Owen[11] presented a thin shell formulation identical to that of Chen[9] for elastoplastic analysis of isotropic plates and shells involving large rotations. Peng and Crisfield[12] also presented a three-node flat triangular shell element identical to that of Chen[9] but employed a corotational formulation in which the rigid-body modes are removed from the total displacements using a procedure similar to that used by Hsiao,[6] thereby enabling the use of very large load increments. Chen,[9] Peric and Owen,[11] and Peng and Crisfield[12] used the same shape functions to compute the tangent stiffness matrix as those used for the linear stiffness matrix, unlike the case of Refs. 3, 4, 6, and 7 in which simpler interpolations were used to compute the tangent stiffness matrix.

The flat shell elements that use the CST or the LST elements to represent the membrane action suffer from in-plane rotational singularity, because these elements do not have drilling degrees of freedom. Though the singularity can be removed by associating a fictitious stiffness with the in-plane rotational degree of freedom, the presence of drilling degrees of freedom is considered essential for the analysis of shells, and elements with such drilling degrees of freedom have been found to exhibit improved membrane response and also a reduced sensitivity to element distortion.[13]

Meek and Tan[14] presented a flat triangular shell element for static analysis of isotropic plates and shells by combining the LST element and a plate bending element with loof nodes (six Gaussian points, two on each edge). In their plate bending element the transverse displacement is expressed in terms of the standard quadratic basis in area coordinates using the corner and midside nodal values. The rotations of the shell normal (β_x, β_y) about local Cartesian coordinates y, x are not expressed using the same quadratic basis because of the existence of a linear combination of the basis, called the neutral function, which is zero at all of the loof nodes. The existense of such neutral functions in rectangular elements had been observed by Gopalacharyulu[15] (in the case of higher-order polynomials at the corners) and Irons[16] (in the case of an incomplete cubic basis at loof nodes), and they suggested that the singularity can be eliminated by expanding the basis by adding an extra node. For a rectangular element with loof nodes, Irons[16] suggested that the centroid be used as the extra node and also presented an expanded basis. Meek and Tan[14] used an expanded basis by adding a cubic term to the standard quadratic basis in area coordinates. They also chose the centroid as the additional node. The normal rotations (β_x, β_y) at the loof nodes and the centroid are eliminated in terms of the rotations of the shell normal about the edges at the loof nodes by imposing Kirchhoff assumptions at a number of discrete points. Meek and Tan[14] claim that by doing so the in-plane rotational singularity is eliminated. Because of the presence of fourth-order terms, a seven-point Gaussian quadrature rule is required to numerically integrate the element stiffness matrix of their element. As a result, nonlinear analysis of large structures using their element might be computationally very expensive.

Recently Poulsen and Damkilde[17] presented a flat triangular shell element by combining the LST element and a plate bending element with loof nodes similar to those of Meek and Tan.[14] The two major differences between the plate bending elements of Meek and Tan[14] and Poulsen and Damkilde[17] are as follows.

1) The seventh term in the expanded basis used by Meek and Tan[14] is unsymmetric in area coordinates, whereas that used by Poulsen and Damkilde[17] preserves symmetry.

2) The basis used by Poulsen and Damkilde[17] to express the transverse displacement has a term $\xi_1\xi_2\xi_3$ in area coordinates called the bubble function, in addition to the standard quadratic basis, with the centroid as the additional node.

Such a basis was expected to give better load distribution and improved results for nonlinear analysis. The final degrees of freedom are the same in both formulations, and the condensation was done by Poulsen and Damkilde[17] as was done by Meek and Tan.[14] Both Meek and Tan[14] and Poulsen and Damkilde[17] have not presented any example on large rotations to demonstrate the performance of the formulation for such problems.

The Allman triangular element[18] is the first successful membrane element based on a displacement model with drilling degrees of freedom. Flat shell elements obtained by combining the Allman element with a suitable plate bending element have been successfully employed for linear analysis.[19–21]

Oral and Barut[22] presented a shear-flexible flat shell element for large deflection and instability analysis of isotropic plates and shells by combining the Allman triangular element and the MIN3 plate bending element of Tessler and Hughes.[23] In the formulation of the MIN3 element, the transverse displacements are expressed in terms of the standard quadratic basis in area coordinates. The shell normal rotations are assumed to vary linearly over the element. The transverse displacements at the midside nodes are eliminated by imposing a constraint that the shear strain be continuous along the element edges. This kind of anisoparametric interpolation and the use of a suitable shear correction factor results in an element that has the correct rank and does not suffer from shear locking even when full numerical integration is used. Oral and Barut[22] employed an updated Lagrangian formulation in which the rigid-body modes are removed from the total displacements using the procedure given by Hsiao.[6]

Madenci and Barut[24] presented a flat shell element for static analysis of composite structures, obtained by combining the flat triangular membrane and bending elements developed by Bergan and Felippa[25] and Felippa and Bergan,[26] respectively, which are based on the formulation termed as free formulation, originally suggested by Bergan and Nygard.[27] In the free formulation, the element stiffness matrix is derived by expressing the requirements of the standard patch test in terms of a set of constraints imposed on the element stiffness matrix, without the need for a variational principle. The presence of in-plane rotations in their formulation[24] eliminates the in-plane rotational singularity. Madenci and Barut[24] employed a corotational form of the updated Lagrangian formulation in which the rigid-body modes are removed using the procedure given by Hsiao.[6] The same element also has been employed by Madenci and Barut[28] for thermal postbuckling analysis of curved composite laminates with cutouts.

In a series of papers, Argyris and Tenek[29–31] presented geometrically nonlinear analysis of isotropic and composite plates and shells subjected to mechanical and thermal loads, using the three-node flat shell element based on the natural-mode technique.

In all of these flat shell elements except those of Bathe and Ho,[4] Fafard et al.,[7] Meek and Tan,[14] and Poulsen and Damkilde,[17] large rotations are handled by removing the rigid-body modes from the total or incremental displacements. Several large-rotation formulations based on isoparametric elements and a total Lagrangian formulation have been presented, in which the large rotations of the shell director are described by using the large-rotation matrix parameterized by three rotation components (e.g., Refs. 32–34) or by using nonlinear trigonometric functions parameterized by two rotation components (e.g., Refs. 35 and 36).

Onate et al.[37] presented a triangular flat shell element for geometrically nonlinear analysis of isotropic shells. Their flat shell element

is a combination of the LST element and a plate bending element (based on Reissner–Mindlin theory) with linear interpolation for the transverse displacement using corner nodes and a linear interpolation for the rotations using midside nodes. Their plate bending element coincides with the plate bending element of Morley[10] in the case of thin plates. Onate et al.[37] have mentioned that their nonlinear formulation is based on Simo's shell theory.[32] No details regarding the formulation as applied to the flat shell element are presented by Onate et al.,[37] nor have they presented any examples involving large rotations to demonstrate the accuracy of the formulation. The formulation of the flat shell element STRI3 of ABAQUS (combination of DKT and CST elements) also is based on description of the motion of the shell director using the large-rotation matrix (parameterized by two rotation components). Not much information is available in the existing literature regarding the formulation or the accuracy of the STRI3 element either for problems involving very large rotations.

In their earlier work, Kapania and Mohan[21] presented static, free-vibration, and thermal analysis of composite plates and shells using a three-node flat triangular shell element that is a combination of the DKT plate bending element and the Allman triangular element. The Allman triangular element used by Oral and Barut[22] was derived using the shape functions suggested by Allman.[18] In the authors' earlier work,[21] the Allman element was derived from the LST element as was done by Ertas et al.[20] using a transformation suggested by Cook.[38]

The motivation for the authors' earlier work was the need for an inexpensive and simple thin shell element that has a better membrane representation and does not suffer from in-plane rotational singularity, shear locking, spurious zero energy modes, etc. The element was intended to be used for two main applications of thin shell structures: control of thermal deformations of a large flexible mirror used in an astronomical telescope[39,40] and nonlinear analysis of large inflatable structures made of woven fabric composites.

The Allman element was chosen for the obvious reason that it simulates the membrane response better than the CST element and does not suffer from in-plane rotational singularity. The Allman triangular element exhibits a zero energy mode when all in-plane nodal translations of the element are zero and all in-plane rotational degrees of freedom of the element are identical. This combination results in singular element stiffness matrix, but this singularity is removed easily by prescribing a value of zero to one of the in-plane rotational degrees of freedom of the entire finite element model.[18] This is in contrast to complex stabilization schemes that are necessary to remove the spurious zero energy modes that are created because of the use of reduced-order numerical integration. In most cases the singularity is automatically removed because of the specified displacement boundary conditions.

The DKT plate bending element was chosen because it has been well established as a reliable thin plate bending element.[5] The shear deformations are neglected, and so it does not suffer from shear locking.

In the present work the flat shell element is extended for geometrically nonlinear analysis of laminated plates and shells so that the element could be used for the analysis of inflatable structures that are expected to undergo large displacements and rotations. The inflatable structures also are expected to undergo large membrane strains. Hence the use of a membrane element such as the CST element is not desirable. Because the membrane element used in the present and earlier works[21,39] exhibits better membrane response than the CST element, it is expected to be more reliable than the CST element.

An updated Lagrangian formulation similar to ULF1 of Fafard et al.[7] is employed in the present study. Several numerical examples are solved to validate the present formulation. The details of the formulation are presented in Sec. II, and the numerical results for a large set of examples are presented in Sec. III.

II. Finite Element Formulation

A. Static Analysis

The nonlinear equations of equilibrium governing the static response of a structure are derived by applying the principle of virtual work for a typical element using a local coordinate system. It is assumed that a known equilibrium configuration C_1 at some time $t = t_1$ is available and that a new configuration C_2 at some time $t = t_2$ has to be determined (Fig. 1).

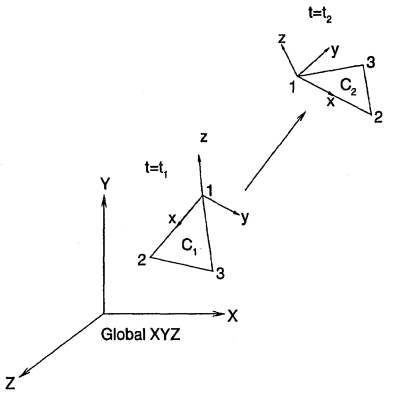

Fig. 1 Motion of a body in a Cartesian coordinate system.

The principle of virtual work can be expressed for a single element as

$$\delta W_e = \delta W_i \tag{1}$$

where δW_e is the virtual work done by external forces and δW_i is the virtual work done by internal forces. The internal virtual work is given by

$$\delta W_i = \int_{C_1} \delta\{\epsilon\}^T \{s\}\, dV \tag{2}$$

where V is the volume of the element in C_1, $\{\epsilon\}$ is the vector of incremental Green–Lagrange strains, and $\{s\}$ is the vector of second Piola–Kirchhoff (PK2) stresses. The PK2 stresses at any time $t_1 < t < t_2$ during the solution process can be decomposed as

$$\{s\} = \{\sigma\} + \{\Delta s\} \tag{3}$$

where $\{\sigma\}$ is the vector of Cauchy stresses in C_1 at time $t = t_1$ and $\{\Delta s\}$ is the vector of incremental PK2 stresses. The incremental Green–Lagrange strains and PK2 stresses in any layer k of a laminated structure are related by the constitutive equations given by

$$\{\Delta s\} = [\bar{Q}_k]\{\epsilon\} \tag{4}$$

where $[\bar{Q}_k]$ is the standard matrix of elastic constants transformed to the element local coordinate system.[21] At the end of the current step, the PK2 stresses in C_1, computed using Eqs. (3) and (4), are converted to Cauchy stresses in C_2 by a series of transformations[41] involving the deformation gradient tensor and the rotation tensor. For small strains, however, it can be shown[7] that, at the end of the current step, the PK2 stresses computed in C_1 are equal to the Cauchy stresses in C_2.

Assuming that the thickness of the structure is small and the incremental rotations are moderate, the variation of strain through the thickness can be expressed as

$$\{\epsilon\} = \{e\} + z\{\kappa\} - \{\epsilon^0\} \tag{5}$$

where $\{e\}$, $\{\kappa\}$, and $\{\epsilon^0\}$ are the vectors of incremental membrane strains, bending strains, and thermal strains, respectively, and are given by

$$\{e\} = \begin{Bmatrix} u_{,x} + \frac{1}{2}(u_{,x}^2 + v_{,x}^2 + w_x^2) \\ v_{,y} + \frac{1}{2}(u_{,y}^2 + v_{,y}^2 + w_{,y}^2) \\ u_{,y} + v_{,x} + u_{,x}u_{,y} + v_{,x}v_{,y} + w_x w_{,y} \end{Bmatrix} \tag{6}$$

$$\{\kappa\} = \{\beta_{x,x} \quad \beta_{y,y} \quad \beta_{x,y} + \beta_{y,x}\}^T \tag{7}$$

$$\{\epsilon^0\} = \{\alpha_x \quad \alpha_y \quad \alpha_{xy}\}_k^T \Delta T \tag{8}$$

where u, v, w are the incremental translations of the midplane of the element; β_x and β_y are the incremental rotations of the normal to

the undeformed midplane about the local y and x axes, respectively; α_x, α_y, and α_{xy} are the coefficients of thermal expansion with respect to the element local coordinate system for the kth layer[21]; and ΔT is the prescribed temperature increment. The local x direction is taken along the side 1-2 of the element with the origin at node 1. The local y axis is perpendicular to side 1-2 of the element and lies in the plane passing through the three nodes of the element. The temperature increment ΔT is assumed to be uniform over the entire element. The present formulation can be extended easily for nonuniform temperature distribution, as was done in the authors' previous work[21] on linear analysis. The internal virtual work now can be expressed as

$$\delta W_i = \int_{C_1} \delta\{\epsilon\}^T\{s\}\,dV = \int_{C_1} (\delta\{\epsilon\}^T\{N\} + \delta\{\kappa\}^T\{M\})\,dA \quad (9)$$

where A is the area of the midplane of the element in C_1 and $\{N\}$ and $\{M\}$ are the force and moment resultants, respectively:

$$\{N, M\} = \int_{-\frac{h}{2}}^{\frac{h}{2}} \{s\}(1, z)\,dz \quad (10)$$

where h is the thickness of the laminate. Using Eqs. (3) and (4), the force and moment resultants can be decomposed as

$$\{N\} = \{N_1\} + \{\Delta N^m\} - \{\Delta N^0\} \quad (11)$$

$$\{M\} = \{M_1\} + \{\Delta M^m\} - \{\Delta M^0\} \quad (12)$$

where $\{N_1\}$, $\{M_1\}$ are the force and moment resultants in C_1 at time $t = t_1$; $\{\Delta N^m\}$, $\{\Delta M^m\}$ are the incremental force and moment resultants due to mechanical stresses; and $\{\Delta N^0\}$, $\{\Delta M^0\}$ are the incremental force and moment resultants due to thermal stresses:

$$\{N_1, M_1\} = \int_{-\frac{h}{2}}^{\frac{h}{2}} \{\sigma\}(1, z)\,dz \quad (13)$$

$$\{\Delta N^m\} = \int_{-\frac{h}{2}}^{\frac{h}{2}} [\bar{Q}_k](\{e\} + z\{\kappa\})\,dz = [A]\{e\} + [B]\{\kappa\} \quad (14)$$

$$\{\Delta M^m\} = \int_{-\frac{h}{2}}^{\frac{h}{2}} [\bar{Q}_k](\{e\} + z\{\kappa\})z\,dz = [B]\{e\} + [D]\{\kappa\} \quad (15)$$

$$\{\Delta N^0, \Delta M^0\} = \int_{-\frac{h}{2}}^{\frac{h}{2}} [\bar{Q}_k]\{\epsilon^0\}(1, z)\,dz \quad (16)$$

where $[A]$, $[B]$, $[D]$ are the standard matrices of elastic constants. All of the integrals are evaluated using a three-point integration scheme in area coordinates.[42] The first variation of the membrane strains can be expressed as

$$\{\delta e\} = \begin{Bmatrix} \delta u_{,x} + u_{,x}\delta u_{,x} + v_{,x}\delta v_{,x} + w_{,x}\delta w_{,x} \\ \delta v_{,y} + u_{,y}\delta u_{,y} + v_{,y}\delta v_{,y} + w_{,y}\delta w_{,y} \\ \delta u_{,y} + \delta v_{,x} + u_{,x}\delta u_{,y} + u_{,y}\delta u_{,x} + v_{,x}\delta v_{,y} + v_{,y}\delta v_{,x} + w_{,x}\delta w_{,y} + w_{,y}\delta w_{,x} \end{Bmatrix} \quad (17)$$

This equation can be rearranged as

$$\{\delta e\} = [G_1]\{\delta u_{,x} \quad \delta u_{,y} \quad \delta v_{,x} \quad \delta v_{,y} \quad \delta w_{,x} \quad \delta w_{,y}\}^T \quad (18)$$

where

$$[G_1] = \begin{bmatrix} 1+u_{,x} & 0 & v_{,x} & 0 & w_{,x} & 0 \\ 0 & u_{,y} & 0 & 1+v_{,y} & 0 & w_{,y} \\ u_{,y} & 1+u_{,x} & 1+v_{,y} & v_{,x} & w_{,y} & w_{,x} \end{bmatrix} \quad (19)$$

The in-plane displacements u and v can be expressed in terms of the nodal quantities as

$$\begin{Bmatrix} u \\ v \end{Bmatrix} = \begin{bmatrix} \{P\}^T & 0 \\ 0 & \{P\}^T \end{bmatrix} \{a_{\text{lst}}\} \quad (20)$$

where $\{a_{\text{lst}}\}$ is the vector of nodal degrees of freedom of the LST element given by $\{a_{\text{lst}}\} = \{u_1, u_2, u_3, u_4, u_5, u_6, v_1, v_2, v_3, v_4, v_5, v_6\}$ and $\{P\}$ is the vector of quadratic shape functions in area coordinates.[21] The shape functions in $\{P\}$ are arranged in such an order that nodes 4, 5, and 6 are at the midpoint of the sides 1-2, 2-3, and 3-1, respectively. The derivatives of the in-plane displacements are given by

$$\begin{Bmatrix} u_{,x} \\ u_{,y} \\ v_{,x} \\ v_{,y} \end{Bmatrix} = \begin{bmatrix} \{P_{,x}\}^T & 0 \\ \{P_{,y}\}^T & 0 \\ 0 & \{P_{,x}\}^T \\ 0 & \{P_{,y}\}^T \end{bmatrix} [T_{\text{lst}}]\{a\} = [B_{\text{lst}}]\{a\} \quad (21)$$

where $\{P_{,x}\}$ and $\{P_{,y}\}$ are the vectors of derivatives of the shape functions with respect to the local x and y coordinates, respectively[21]; the matrix $[T_{\text{lst}}]$, which is given in Ref. 21, is used to express the nodal degrees of the LST element $\{a_{\text{lst}}\}$ in terms of the nodal degrees of freedom of the shell element $\{a\}$ as $\{a_{\text{lst}}\} = [T_{\text{lst}}]\{a\}$, where $\{a\}^T = \{u_1, v_1, w_1, \theta_{x_1}, \theta_{y_1}, \theta_{z_1}, u_2, v_2, w_2, \theta_{x_2}, \theta_{y_2}, \theta_{z_2}, u_3, v_3, w_3, \theta_{x_3}, \theta_{y_3}, \theta_{z_3}\}$.

In the case of the DKT element, the transverse displacement w is not explicitly defined over the interior of the element. The derivatives $w_{,x}$ and $w_{,y}$ at the integration points (located at the interior of the element) can be obtained using a linear interpolation in terms of the nodal values. However, this kind of interpolation required a very fine mesh and small load steps, probably because of the nonconformal nature of the derivatives along the element sides. Past experience has shown that evaluating the derivatives from a linear interpolation for w using the nodal values gives better results.[7] The same approach is followed here. In area coordinates, w is expressed as $w(\xi, \eta) = (1 - \xi - \eta)w_1 + \xi w_2 + \eta w_3$, from which the derivatives can be obtained as

$$\begin{Bmatrix} w_{,x} \\ w_{,y} \end{Bmatrix} = \frac{1}{2A} \begin{bmatrix} -b_2 - b_3 & b_2 & b_3 \\ -c_2 - c_3 & c_2 & c_3 \end{bmatrix} [T_w]\{a\} = [B_w]\{a\} \quad (22)$$

where A is the area of the midplane of the element in C_1, $b_i = y_j - y_k$, $c_i = x_k - x_j$, and $[T_w]$ is used to express $\{w_1 \ w_2 \ w_3\}^T$ in terms of $\{a\}$ as $\{w_1 \ w_2 \ w_3\}^T = [T_w]\{a\}$. The transformation matrix $[T_w]$ is made of zeroes and ones and its determination is straightforward. Combining Eqs. (21) and (22), the first variation of the membrane strains can be expressed as

$$\{\delta e\} = [G_1][G_2]\{\delta a\} \quad (23)$$

where $[G_2]$ is a matrix of size 6×18 with the first four rows made of $[B_{\text{lst}}]$ and the last two rows made of $[B_w]$. The normal rotations β_x and β_y can be expressed in terms of the nodal degrees of freedom of the DKT element as

$$\beta_x = (1/2A)[H_x(\xi, \eta)]\{a_{\text{dkt}}\}, \qquad \beta_y = (1/2A)[H_y(\xi, \eta)]\{a_{\text{dkt}}\} \quad (24)$$

where $\{a_{\text{dkt}}\}$ is the vector of nodal degrees of freedom of the DKT element given by $\{a_{\text{dkt}}\}^T = \{w_1 \ \theta_{x_1} \ \theta_{y_1} \ w_2 \ \theta_{x_2} \ \theta_{y_2} \ w_3 \ \theta_{x_3} \ \theta_{y_3}\}$, $[H_x]$ and $[H_y]$ are the vectors of shape functions given by Batoz et al.[5] These shape functions have been reordered such that nodes 4, 5, and 6 are at the midpoint of the sides 1-2, 2-3, and 3-1, respectively. This can be accomplished easily by replacing the subscripts 4, 5, and 6 with 5, 6, and 4, respectively. This reordering has been done to match the order of the nodes with that of the LST element to avoid confusion while coding. The bending strains now can be expressed as

$$\{\kappa\} = \frac{1}{2A} \begin{bmatrix} b_2 H^T_{x,\xi} + b_3 H^T_{x,\eta} \\ c_2 H^T_{y,\xi} + c_3 H^T_{y,\eta} \\ c_2 H^T_{x,\xi} + c_3 H^T_{x,\eta} + b_2 H^T_{y,\xi} + b_3 H^T_{y,\eta} \end{bmatrix} [T_{\text{dkt}}]\{a\} = [B_{\text{dkt}}]\{a\} \quad (25)$$

where $H_{x,\xi}$, $H_{x,\eta}$, $H_{y,\xi}$, $H_{y,\eta}$ are the derivatives of the shape functions given by Batoz et al.,[5] which also have been reordered as mentioned earlier. The matrix $[T_{\mathrm{dkt}}]$, which is given in Ref. 19, is used to express $\{a_{\mathrm{dkt}}\}$ in terms of $\{a\}$ as $\{a_{\mathrm{dkt}}\} = [T_{\mathrm{dkt}}]\{a\}$. The external virtual work can be expressed as

$$\delta W_e = \{\delta a\}^T \{f\} \tag{26}$$

where $\{f\}$ is the element external force vector (due to mechanical loads). The equations of equilibrium at the element level can be expressed as

$$\{g\} = \{q\} - \{f\} = \int_{C_1} \left([G_2]^T[G_1]^T\{N\} + [B_{\mathrm{dkt}}]^T\{M\}\right) \mathrm{d}A - \{f\} = 0 \tag{27}$$

where $\{q\}$ is the element internal force vector. The element internal and external force vectors thus obtained in the element local coordinates are converted to the global coordinates using the standard coordinate transformation[43] and are assembled to obtain the global internal force vector $\boldsymbol{q}$ and external force vector $\boldsymbol{f}$. In the rest of the section, vectors and matrices in the global coordinate system are denoted in boldface.

The equilibrium equations of the entire finite element model in the global Cartesian coordinate system at any time t can be written as $\boldsymbol{g}_t = \boldsymbol{q}_t - \boldsymbol{f}_t = 0$, where $\boldsymbol{g}$ is the residue of or the imbalance between the internal and external forces. In all numerical examples, only configuration-independent concentrated loads are considered. Hence, the external global load vector $\boldsymbol{f}$ can be obtained just by prescribing the global nodal forces. Also, the thermal and mechanical loads are not applied simultaneously. The nonlinear equations of equilibrium are solved using the Newton–Raphson method, an iterative or step-by-step process in which a linearized form of the equilibrium equations are solved in each step. The Newton–Raphson method is illustrated in Ref. 44 using load control for mechanical and thermal loads separately. Details of arc-length control can be found in Ref. 45. Assuming that a known equilibrium configuration exists at some time t_1 the equations of equilibrium at some time $t_1 + \Delta t$ can be linearized using the truncated Taylor-series expansion about the known configuration at time t_1 as

$$\boldsymbol{g}_{t_1+\Delta t} = \boldsymbol{q}_{t_1} + \left(\frac{\partial \boldsymbol{q}}{\partial \boldsymbol{a}}\right)_{t_1} \delta \boldsymbol{a} - \boldsymbol{f}_{t_1+\Delta t} = \boldsymbol{q}_{t_1} + [\boldsymbol{K}]\delta \boldsymbol{a} - \boldsymbol{f}_{t_1+\Delta t} \tag{28}$$

where $[\boldsymbol{K}]$ is the global tangent stiffness matrix, which is obtained by transforming the local element stiffness matrices $[k]$ [obtained by taking the derivative of the element internal force vector $\{q\}$ in Eq. (27) with respect to $\{a\}$] and assembling them in the standard way. The derivative of the terms in Eq. (27) is obtained using the chain rule

$$\delta(\,) = \frac{\partial(\,)}{\partial\{a\}}\delta\{a\}$$

Using Eqs. (11), (12), (14), (15), (23), and (25), the derivatives of $\{N\}$ and $\{M\}$ w.r.t. $\{a\}$ can be obtained readily as

$$\begin{aligned} \frac{\partial\{N\}}{\partial\{a\}} &= [A][G_1][G_2] + [B][B_{\mathrm{dkt}}] \\ \frac{\partial\{M\}}{\partial\{a\}} &= [B][G_1][G_2] + [D][B_{\mathrm{dkt}}] \end{aligned} \tag{29}$$

The variation of the product $[G_2]^T[G_1]^T\{N\}$ is given by

$$\delta\left([G_2]^T[G_1]^T\{N\}\right) = [G_2]^T\left(\delta[G_1]^T\right)\{N\} + [G_2]^T[G_1]^T\delta\{N\} \tag{30}$$

Using the special property of the matrix $[G_1]$ (Ref. 46, p. 294), the product $(\delta[G_1]^T)\{N\}$ can be expressed as

$$\left(\delta[G_1]^T\right)\{N\} = \begin{bmatrix} \hat{N} & 0 & 0 \\ 0 & \hat{N} & 0 \\ 0 & 0 & \hat{N} \end{bmatrix} [G_2]\delta\{a\} \tag{31}$$

where n_x, n_y, and n_{xy} are the components of $\{N\}$ and

$$\hat{N} = \begin{bmatrix} n_x & n_{xy} \\ n_{xy} & n_y \end{bmatrix}$$

The derivative of $[G_2]^T[G_1]^T\{N\}$ with respect to $\{a\}$ can be obtained easily using Eqs. (30) and (31) and the chain rule. The element tangent stiffness matrix $[k]$ now can be expressed as

$$\begin{aligned} [k] = \int_{C_1} \Big(& [G_2]^T[G_1]^T[A][G_1][G_2] + [B_{\mathrm{dkt}}]^T[D][B_{\mathrm{dkt}}] \\ & + [B_{\mathrm{dkt}}]^T[B][G_1][G_2] + [G_2]^T[G_1]^T[B][B_{\mathrm{dkt}}] \\ & + [G_2]^T \begin{bmatrix} \hat{N} & 0 & 0 \\ 0 & \hat{N} & 0 \\ 0 & 0 & \hat{N} \end{bmatrix} [G_2] \Big) \mathrm{d}A \end{aligned} \tag{32}$$

B. Dynamic Analysis

As in the case of static analysis, it is assumed that a known equilibrium configuration exists at some time t_1 and the solution at some time $t_1 + \Delta t$ has to be determined. The equations of equilibrium governing the dynamic response of a structure at time $t_1 + \Delta t$ can be expressed as $M\ddot{a}_{t_1+\Delta t} + \boldsymbol{q}_{t_1+\Delta t} = \boldsymbol{f}_{t_1+\Delta t}$, where M is the mass matrix, $\boldsymbol{q}$ is the internal force, and $\boldsymbol{f}$ is the externally applied force. A consistent mass matrix as described in the authors' previous work[21] is employed in the present study. The equations of equilibrium are solved using the Newton–Raphson method in combination with the Newmark integration scheme. The reader is directed to Ref. 1 for details of the algorithm.

III. Numerical Examples

Several numerical examples were solved to verify the accuracy of the present formulation and the results are presented in this section. All examples were solved using the full Newton–Raphson method with load control or arc-length control.[45] The results obtained using the present formulation are compared with the results available in the existing literature and those obtained using the STRI3, S4R, and S4R5 elements of ABAQUS using the same solution procedure that is used with the present formulation. The STRI3 element is a three-node flat triangular shell element obtained by combining the DKT plate bending element and the CST membrane element. The S4R element is a four-node doubly curved shell element with reduced integration, for thin or thick shells, and the S4R5 element is similar to the S4R element but is applicable only for thin shells. In Figs. 3–7 and 11, the mesh shown for the initial geometry is only for illustrative purpose and is not the same as the actual mesh used for the computation.

A. Static Response Analysis

The results for the static response analysis (snap-back behavior) of an anisotropic hinged cylindrical panel are given in Ref. 44. To demonstrate the accuracy of the present formulation for problems involving large rotations, five standard problems have been considered.

1. *Cantilever Beam Under a Tip Moment*

The geometry and material properties used are those given by Hsiao.[6] The applied bending moment ($2000\,\pi$ Nm) at the tip causes the beam to deform into a full circle. In Fig. 2, the results obtained using the present formulation (using load control in 50 steps and a total of 200 iterations) are compared with those obtained using STRI3, S4R5, and S4R elements of ABAQUS. The present results are in good agrreement with those obtained using STRI3 and S4R elements. The results obtained using the S4R5 element show slight deviation from the rest of the results for $4200 < M < 6000$ Nm.

2. *Clamped Cylindrical Shell Under Pinching Loads at the Apex*

The geometry and material properties are those given by Brank et al.[36] The analysis was performed until the deflection under the load was just about equal to the radius of the cylinder. The load-deflection path was traced using arc-length control in 32 increments with a total of 120 iterations. Though the response does not show any instabilities, arc-length control has been used because the convergence is faster in the case of arc-length control than load control. In Fig. 3, the results obtained using the present formulation are compared with

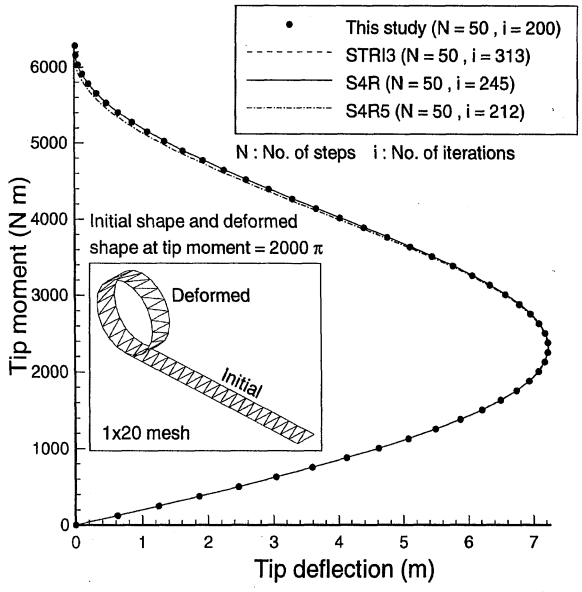

Fig. 2 Cantilever beam under a tip moment.

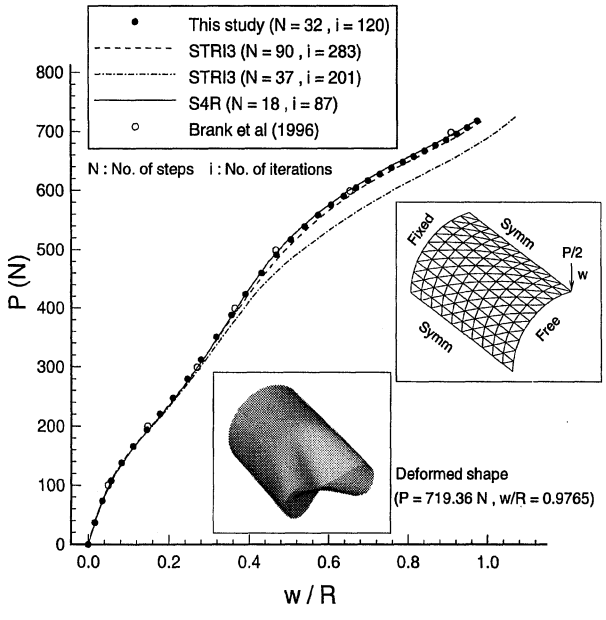

Fig. 3 Clamped cylindrical shell under pinching loads (quarter shell model, 30 × 30 mesh).

those obtained using STRI3, S4R, and those of Brank et al.[36] The STRI3 element showed severe convergence problem for $P > 500$ N when load control was used. Though large load increments could be used up to $P = 500$ N, the load increments were automatically cut down for $P > 500$ N, resulting in at least 100 steps. When arc-length control was used, the STRI3 element showed extreme sensitivity to the size of the arc-length increments. Only the results obtained using the arc-length control are presented in the case of the STRI3 element. The flat shell element of the present study and S4R did not show such problems. As can be seen from Fig. 3, the results obtained using the STRI3 element in 37 increments do not agree well with the rest of the results. The present results agree well with those of Brank et al.,[36] S4R, and STRI3 (obtained using 90 increments).

3. Cylindrical Shell with Free Ends Under Stretching Loads at the Apex

The geometry and material properties are those given by Brank et al.[36] Two distinct zones of stiff and soft behavior can be identified from the load deflection curve (Fig. 4). Most of the results in the existing literature show good agreement only in the soft zone. In Fig. 4, the results obtained using the present formulation (arc-length control in 25 steps with a total of 95 iterations) are compared with those of Brank et al.[36] and those obtained using the S4R and S4R5 elements

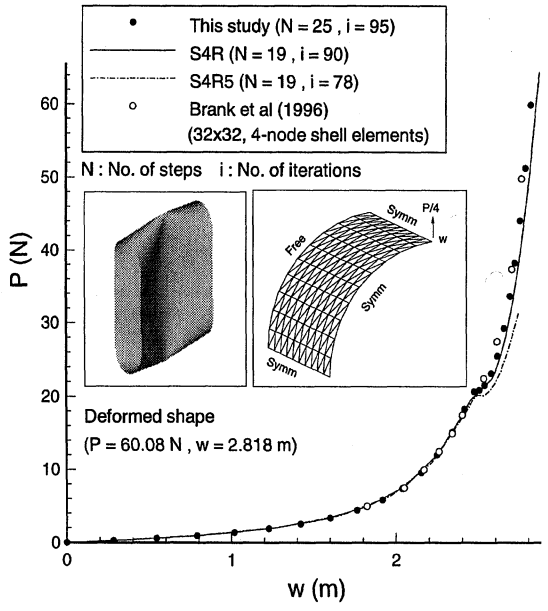

Fig. 4 Cylindrical shell with free ends under stretching loads (one-eighth shell model, 20 × 20 mesh).

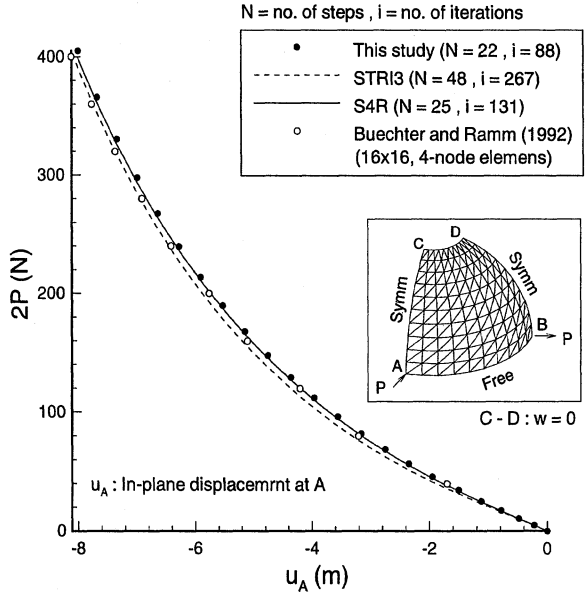

Fig. 5 Hemispherical shell under pinching and stretching loads (u at point a, quarter-shell model, 40 × 40 mesh).

of ABAQUS. The present results are in good agreement with those of Brank et al.[36] and S4R in both the stiff and the soft zones. The S4R5 element failed to proceed in the same direction for $P > 32$ N.

4. Hemispherical Shell with a Hole Under Pinching and Stretching Loads

The geometry and material properties are those given by Buechter and Ramm.[47] In the present study, the transverse displacement (w) along the hole (Fig. 5) is constrained to prevent the rigid-body motion, which otherwise is not suppressed by the symmetry conditions shown in Fig. 5. The results obtained using the present formulation (arc-length control in 22 steps with a total of 88 iterations) are compared with those of Buechter and Ramm[47] and those obtained using STRI3 and S4R elements in Figs. 5 and 6. The present results are in good agreement with those of Buechter and Ramm[47] and S4R. The results obtained using the STRI3 element for the transverse displacement (Fig. 6) do not agree well with the present results and those obtained using S4R.

5. Ring Plate Under a Line Load at the Free Edge

The geometry and material properties are those given by Buechter and Ramm.[47] The results obtained using the present formulation

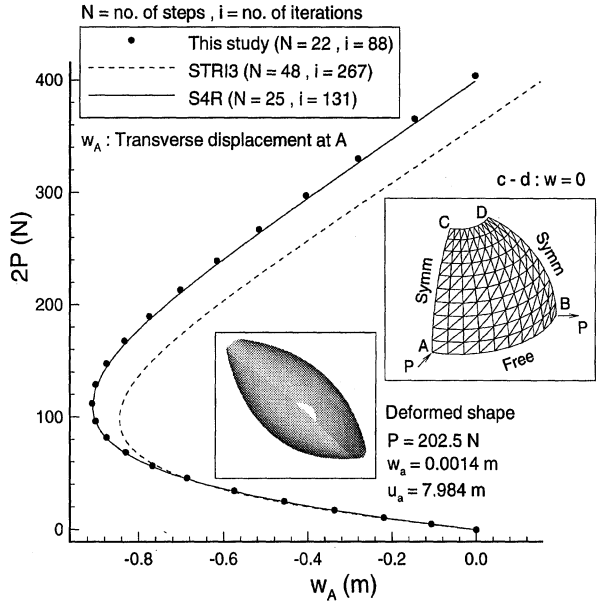

Fig. 6 Hemispherical shell under pinching and stretching loads (w at point a, quarter shell model, 40 × 40 mesh).

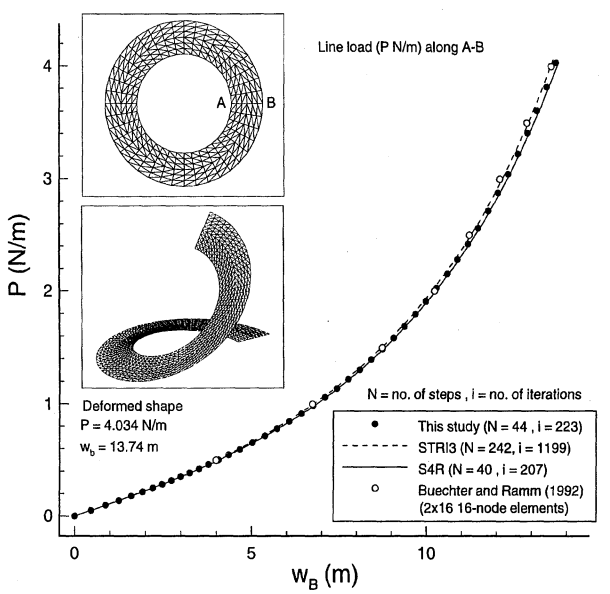

Fig. 7 Ring plate under line load at the free edge (full plate, 10 × 80 mesh).

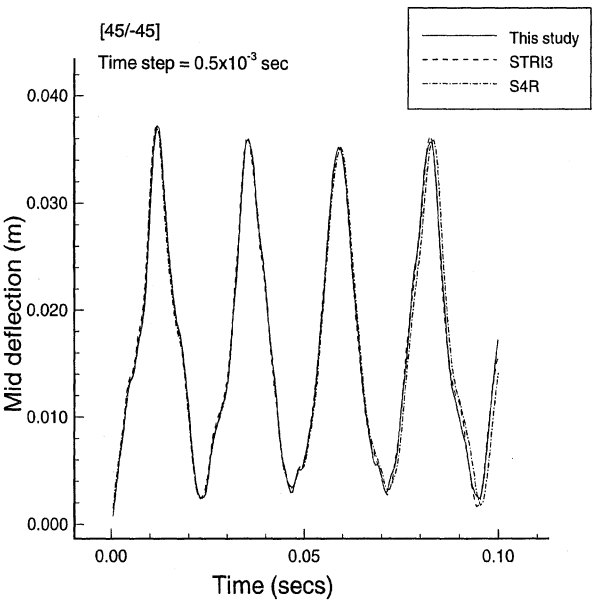

Fig. 8 Dynamic analysis of an anisotropic ([45/−45]) hinged cylindrical panel under a concentrated load at the center.

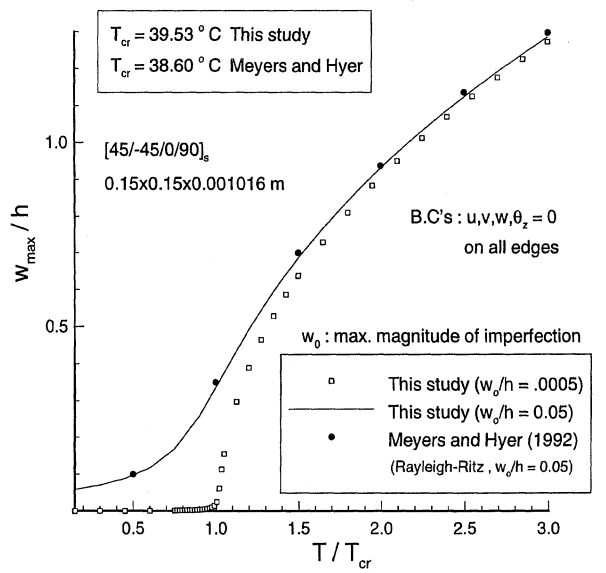

Fig. 9 Thermal postbuckling analysis of a simply supported square plate under uniform temperature rise (full plate, 16 × 16 mesh).

(arc-length control in 44 steps and 223 iterations) are compared with those of Buechter and Ramm[47] and those obtained using the S4R and STRI3 elements in Fig. 7. The present results are in good agreement with the rest of the results. As in the case of the pinched cylindrical shell, the STRI3 element showed some convergence problems. Though large initial increments were used (in arc-length control) the increments were cut down several times during the course of the analysis, resulting in 242 increments with a total of 1199 iterations. The total number of iterations used in the case of the present formulation or S4R are smaller than the total number of increments used in the case of the STRI3 element.

B. Dynamic Response Analysis

The dynamic response analysis of an antisymmetric angle ply laminated ([45/−45]) hinged cylindrical panel of thickness 0.0126 m under a centrally applied load of 1600 N was performed. The geometry and material properties are those given by Brank et al.[36] The density and time step are 1000 kg/m^3 and 0.5 × 10^{-3}, respectively. The force was applied at time $t = 0$ and held constant. The results obtained using the present formulation are compared with those obtained using the STRI3 and S4R elements (using same time step) in Fig. 8 and are in good agreement with each other.

C. Thermal Postbuckling Analysis

The thermal postbuckling analysis of a simply supported symmetrically laminated imperfect square plate and an antisymmetric angle ply laminated clamped cylindrical panel subject to a uniform temperature increase was performed. The material properties used for the plate are those given by Meyers and Hyer[48] and the imperfections considered are in the form of the first buckling mode. The bifurcation behavior of the perfect plate at the critical temperature was simulated by adding a very small amount of imperfection, with a maximum magnitude of 0.0005 times the thickness of the plate. The critical temperature (39.491°C) was determined by performing a linear thermal buckling analysis. The same shape functions that were used to compute the so-called consistent mass matrix in the authors' earlier work[21] have been used to compute the geometric stiffness matrix. The eigenvalue problem was solved using a subspace iteration method. The material properties used for the clamped cylindrical panel are those given by Huang and Tauchert,[49] and the geometry is the same as that used in the dynamic analysis except that the thickness used in this case is 0.00254 m.

The results for thermal postbuckling analysis of the square plate are given in Fig. 9 along with the Rayleigh–Ritz solution of Meyers and Hyer[48] and are in good agreement. The results given in Fig. 9 are nondimensionalized with respect to the critical buckling

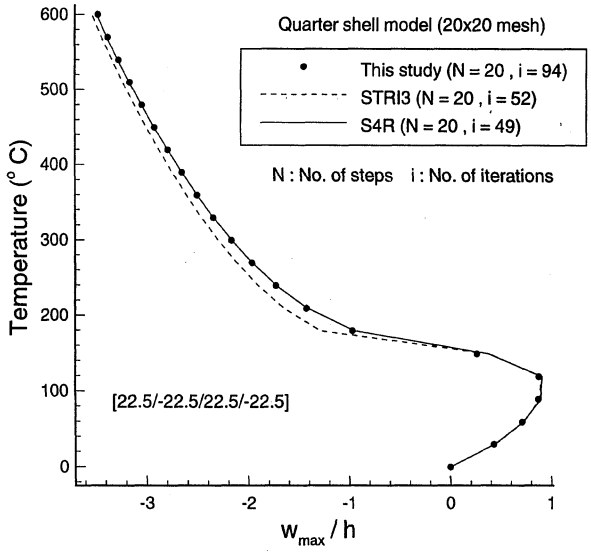

Fig. 10 Thermal postbuckling analysis of a clamped cylindrical panel under uniform temperature rise.

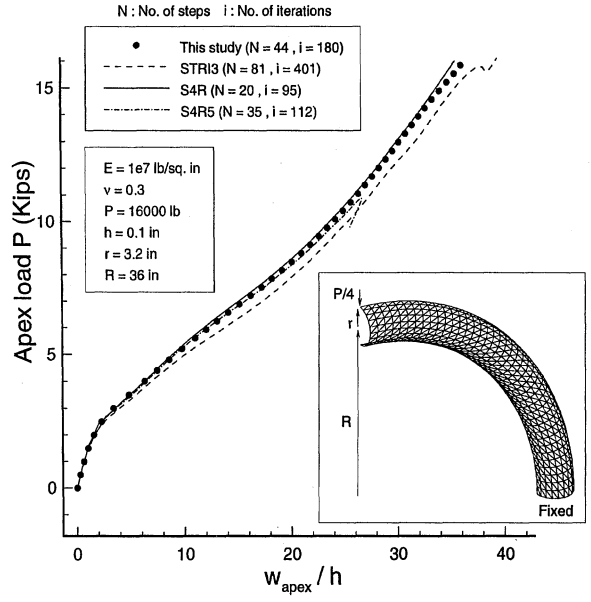

Fig. 11 Circular arch under apex load (quarter arch model, 30 × 100 mesh).

temperature (38.6°C) given by Meyers and Hyer.[48] The response of the imperfect plate closely follows the simulated response of the perfect plate as in the case of the results presented by Meyers and Hyer.[48] The results for the response of a clamped cylinder under uniform temperature rise are given in Fig. 10 along with those obtained using the STRI3 and S4R elements. The present results are in excellent agreement with those obtained using the S4R element, whereas the results obtained using the STRI3 element do not agree well with the present results or those obtained using S4R.

D. Analysis of a Circular Arch

Static analysis of an isotropic circular arch under a concentrated apex load was performed. The results are given in Figs. 11 (30 × 100 mesh, 18,786 degrees of freedom) and 12 (50 × 100 mesh, 30,906 degrees of freedom) along with those obtained using STRI3, S4R5, and S4R elements. As can be seen from Fig. 11, the results obtained using the present formulation are in good agreement with those obtained using the S4R element except for a slight deviation for $P > 15{,}000$ lb. The results obtained using the S4R5 element are in good agreement with the present results and those obtained using the S4R element until $P = 11{,}000$ lb, after which the S4R5 element shows a snap-through behavior. The results obtained using the STRI3 element do not agree well with the rest of the results. The STRI3 element also shows a snap-through behavior at a later stage.

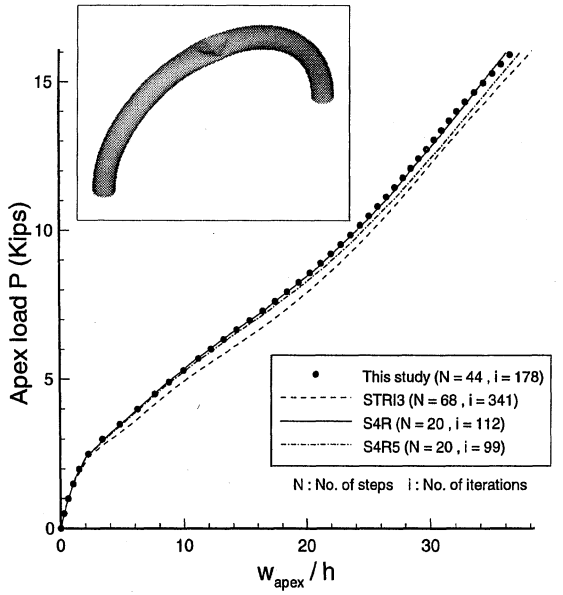

Fig. 12 Circular arch under apex load (quarter arch model, 50 × 100 mesh).

As in the case of the pinched-cylinder problem the STRI3 element also showed some convergence problems. Not much difference was noticed between the results obtained using the present formulation with 30 × 100 mesh and 50 × 100 mesh. The agreement of the present results with those obtained using the S4R element is much better in the case of a 50 × 100 mesh (Fig. 12). Both STRI3 and S4R5 elements gave a stable solution when a 50 × 100 mesh was used but the results do not agree well with those obtained using the present formulation or the S4R element. As can be seen from Fig. 12, the arch undergoes large deformation only in the region around the apex. Hence, a finer grid could have been used only around the apex. Such grid stretching was not done because the main aim of the study was only to assess the accuracy of the formulation.

IV. Summary and Conclusions

Geometrically nonlinear analysis of isotropic and composite plates and shells using a three-node flat triangular shell element was presented. The flat shell element is a combination of discrete Kirchhoff theory (DKT) plate bending element and a membrane element similar to the Allman element but derived from the linear strain triangular (LST) element. Several numerical examples involving small and large rotations were solved to validate the accuracy of the present formulation. The results obtained using the present formulation agreed well with those available in the existing literature and those obtained using the S4R element of the commercial finite element software ABAQUS. In the case of problems involving large rotations, more steps were required for the analysis using the present element than were required by the S4R element or elements in the existing literature based on a large-rotation theory, but the analysis is not computationally expensive because of the simplicity of the formulation. The present formulation did not show any convergence problems like that of the flat shell element STRI3 and also did not require extremely fine meshes to obtain a stable solution like the STRI3 and S4R5 elements. The present formulation does not suffer from in-plane rotational singularity, spurious zero energy modes, shear-locking, etc., and is very reliable for nonlinear analysis of large flexible structures.

Acknowledgments

The support provided for this research by Grant DAAH04-95-1-0175 from the Army Research Office with Gary Anderson as the Grant Monitor is greatly appreciated. We would like to thank B. Grossman, Department Head, Aerospace and Ocean Engineering, for providing considerable computational resources. We also would like to thank Raymond Plaut (Department of Civil Engineering), Daniel Hammerand, and Jing Li (Department of Aerospace and Ocean Engineering) for the valuable discussions held during the course of this research.

References

[1]Bathe, K. J., Ramm, E., and Wilson, E. L., "Finite Element Formulations for Large Deformation Dynamic Analysis," *International Journal for Numerical Methods in Engineering*, Vol. 9, 1975, pp. 353–386.

[2]Argyris, J. H., Dunne, P. C., Malejannakis, G. A., and Schelkle, E., "A Simple Triangular Facet Shell Element with Applications to Linear and Non-Linear Equilibrium and Elastic Stability Problems," *Computer Methods in Applied Mechanics and Engineering*, Vol. 10, 1977, pp. 371–403.

[3]Horrigmoe, G., and Bergan, P. G., "Nonlinear Analysis of Free-Form Shells by Flat Finite Elements," *Computer Methods in Applied Mechanics and Engineering*, Vol. 16, 1978, pp. 11–35.

[4]Bathe, K. J., and Ho, L. W., "A Simple and Effective Element for Analysis of General Shell Structures," *Computers and Structures*, Vol. 13, 1981, pp. 673–681.

[5]Batoz, J. L., Bathe, K. J., and Ho, L. W., "A Study of Three-Node Triangular Plate Bending Elements," *International Journal for Numerical Methods in Engineering*, Vol. 15, 1980, pp. 1771–1812.

[6]Hsiao, K. M., "Nonlinear Analysis of General Shell Structures by Flat Triangular Shell Element," *Computers and Structures*, Vol. 25, No. 5, 1987, pp. 665–675.

[7]Fafard, M., Dhatt, G., and Batoz, J. L., "A New Discrete Kirchhoff Plate/Shell Element with Updated Procedures," *Computers and Structures*, Vol. 31, 1989, pp. 591–606.

[8]Dhatt, G., Marcotte, L., and Matte, Y., "A New Triangular Discrete Kirchhoff Plate Shell Element," *International Journal for Numerical Methods in Engineering*, Vol. 23, 1986, pp. 453–470.

[9]Chen, K. K., "A Triangular Plate Finite Element for Large-Displacement Elastic-Plastic Analysis of Automobile Structural Components," *Computers and Structures*, Vol. 10, 1979, pp. 203–215.

[10]Morley, L. S. D., "The Constant-Moment Plate Bending Element," *Journal of Strain Analysis*, Vol. 6, No. 1, 1971, pp. 20–24.

[11]Peric, D., and Owen, D. R. J., "The Morley Thin Shell Finite Element for Large Deformations Problems: Simplicity Versus Sophistication," *Proceedings of the International Conference on Nuclear Engineering Computations*, Pineridge, Swansea, Wales, UK, 1991, pp. 121–142.

[12]Peng, X., and Crisfield, M. A., "A Consistent Co-Rotational Formulation for Shells Using the Constant Stress/Constant Moment Triangle," *International Journal for Numerical Methods in Engineering*, Vol. 35, 1992, pp. 1829–1847.

[13]Knight, N. F., Jr., "Raasch Challenge for Shell Elements," *AIAA Journal*, Vol. 35, No. 2, 1997, pp. 375–381.

[14]Meek, J. L., and Tan, H. S., "Instability Analysis of Thin Plates and Arbitrary Shells Using a Faceted Shell Element with Loof Nodes," *Computer Methods in Applied Mechanics and Engineering*, Vol. 57, 1986, pp. 143–170.

[15]Gopalacharyulu, S., "A Higher Order Conforming Rectangular Plate Element," *International Journal for Numerical Methods in Engineering*, Vol. 6, 1973, pp. 305–308.

[16]Irons, B. M., "Comment on a Higher Order Conforming Rectangular Plate Element by S. Gopalacharyulu," *International Journal for Numerical Methods in Engineering*, Vol. 6, 1973, pp. 308, 309.

[17]Poulsen, P. N., and Damkilde, L., "A Flat Triangular Shell Element with Loof Nodes," *International Journal for Numerical Methods in Engineering*, Vol. 39, 1996, pp. 3867–3887.

[18]Allman, D. J., "A Compatible Triangular Element Including Vertex Rotations for Plane Elasticity Analysis," *Computers and Structures*, Vol. 19, No. 1–2, 1984, pp. 1–8.

[19]Chen, H. C., "Evaluation of Allman Triangular Membrane Element Used in General Shell Analysis," *Computers and Structures*, Vol. 43, No. 5, 1992, pp. 881–887.

[20]Ertas, A., Krafcik, J. T., and Ekwaro-Osire, S., "Performance of an Anisotropic Allman/DKT 3-Node Thin Triangular Flat Shell Element," *Composites Engineering*, Vol. 2, No. 4, 1992, pp. 269–280.

[21]Kapania, R. K., and Mohan, P., "Static, Free Vibration and Thermal Analysis of Composite Plates and Shells Using a Flat Triangular Shell Element," *Computational Mechanics*, Vol. 17, 1996, pp. 343–357.

[22]Oral, S., and Barut, A., "A Shear-Flexible Facet Shell Element for Large Deflection and Instability Analysis," *Computer Methods in Applied Mechanics and Engineering*, Vol. 93, 1991, pp. 415–431.

[23]Tessler, A., and Hughes, T. J. R., "A Three-Node Mindlin Plate Element with Improved Transverse Shear," *Computer Methods in Applied Mechanics and Engineering*, Vol. 50, 1985, pp. 71–101.

[24]Madenci, E., and Barut, A., "A Free Formulation-Based Flat Shell Element for Nonlinear Analysis of Thin Composite Structures," *International Journal for Numerical Methods in Engineering*, Vol. 37, 1994, pp. 3825–3842.

[25]Bergan, P. G., and Felippa, C. A., "A Triangular Membrane Element with Rotational Degrees of Freedom," *Computer Methods in Applied Mechanics and Engineering*, Vol. 50, 1985, pp. 24–69.

[26]Felippa, C. A., and Bergan, P. G., "A Triangular Bending Element Based on Energy Orthogonal Free Formulation," *Computer Methods in Applied Mechanics and Engineering*, Vol. 61, 1987, pp. 129–160.

[27]Bergan, P. G., and Nygard, M. K., "Finite Elements with Increased Freedom in Choosing Shape Functions," *International Journal for Numerical Methods in Engineering*, Vol. 20, 1984, pp. 643–663.

[28]Madenci, E., and Barut, A., "Thermal Postbuckling Analysis of Cylindrically Curved Composite Laminates with a Hole," *International Journal for Numerical Methods in Engineering*, Vol. 37, 1994, pp. 2073–2091.

[29]Argyris, J., and Tenek, L., "Linear and Geometrically Nonlinear Bending of Isotropic and Multilayered Composite Plates by the Natural Node Method," *Computer Methods in Applied Mechanics and Engineering*, Vol. 113, 1994, pp. 207–251.

[30]Argyris, J., and Tenek, L., "High-Temperature Bending, Buckling and Postbuckling of Laminated Composite Plates Using the Natural Mode Method," *Computer Methods in Applied Mechanics and Engineering*, Vol. 117, 1994, pp. 105–142.

[31]Argyris, J., and Tenek, L., "Postbuckling of Composite Laminates Under Compressive Load and Temperature," *Computer Methods in Applied Mechanics and Engineering*, Vol. 128, 1995, pp. 49–80.

[32]Simo, J. C., and Fox, D. D., "On a Stress Resultant Geometrically Exact Shell Model, Part I. Formulation and Optimal Parametrization," *Computer Methods in Applied Mechanics and Engineering*, Vol. 72, 1989, pp. 267–304.

[33]Parisch, H., "An Investigation of a Finite Rotation Four Node Assumed Strain Shell Element," *International Journal for Numerical Methods in Engineering*, Vol. 31, 1991, pp. 127–150.

[34]Ibrahimbegovic, A., "Stress Resultant Geometrically Nonlinear Shell Theory with Drilling Rotations—Part I: A Consistent Formulation," *Computer Methods in Applied Mechanics and Engineering*, Vol. 118, 1994, pp. 265–284.

[35]Surana, K. S., "Geometrically Nonlinear Formulation for the Curved Shell Elements," *International Journal for Numerical Methods in Engineering*, Vol. 19, 1983, pp. 581–615.

[36]Brank, B., Peric, D., and Damjanic, B., "On Implementation of Non-Linear Four Node Shell Element for Thin Multilayered Elastic Shells," *Computational Mechanics*, Vol. 16, 1995, pp. 341–358.

[37]Onate, E., Zarate, F., and Flores, F., "A Simple Triangular Element for Thick and Thin Plate and Shell Analysis," *International Journal for Numerical Methods in Engineering*, Vol. 37, 1994, pp. 2569–2582.

[38]Cook, R. D., "On the Allman Triangle and a Related Quadrilateral Element," *Computers and Structures*, Vol. 22, 1986, pp. 1065–1067.

[39]Mohan, P., Kapania, R. K., and Jakubowski, A., "Control of Thermal Deformation of a Spherical Mirror Segment," AIAA Paper 96-4154, 1996.

[40]Jakubowski, A. K., Mohan, P., Kapania, R. K., Crissafulli, P., and Hammerand, D., "8-m UV/Visible/IR Space Telescope," *Proceedings of SPIE—The International Society for Optical Engineering*, Vol. 2478, 1995, pp. 20–34.

[41]Kleiber, M., *Incremental Finite Element Modeling in Non-Linear Solid Mechanics*, Wiley, New York, 1989.

[42]Yang, T. Y., *Finite Element Structural Analysis*, Prentice–Hall, Englewood Cliffs, NJ 1986.

[43]Zienkiewicz, O. C., *The Finite Element Method*, 3rd ed., McGraw–Hill, New York, 1977.

[44]Mohan, P., and Kapania, R. K., "Geometrically Nonlinear Analysis of Composite Plates and Shells Using a Flat Triangular Shell Element," *Proceedings of the AIAA/ASME/ASCE/AHS/ASC 38th Structures, Structural Dynamics, and Materials Conference* (Kissimmee, FL), AIAA, Reston, VA, pp. 2347–2361 (AIAA Paper 97-1233).

[45]Crisfield, M. A., "A Fast Incremental/Iterative Solution Procedure That Handles Snap-Through," *Computers and Structures*, Vol. 13, 1981, pp. 55–62.

[46]Zienkiewicz, O. C., and Taylor, R. L., *The Finite Element Method*, 4th ed., Vol. 2, McGraw–Hill, New York, 1989.

[47]Buechter, N., and Ramm, E., "Shell Theory Versus Degeneration—A Comparison in Large Rotation Finite Element Analysis," *International Journal for Numerical Methods in Engineering*, Vol. 34, 1992, pp. 39–59.

[48]Meyers, C. A., and Hyer, M. W., "Thermally-Induced, Geometrically Nonlinear Response of Symmetrically Laminated Composite Plates," *Composites Engineering*, Vol. 2, No. 1, 1992, pp. 3–20.

[49]Huang, N. N., and Tauchert, T. R., "Large Deflections of Laminated Cylindrical and Doubly Curved Panels Under Thermal Loading," *Computers and Structures*, Vol. 41, No. 2, 1991, pp. 303–312.

A. D. Belegundu
Associate Editor